Obtaining the size distribution of fault gouges with polydisperse bearings

Pedro G. Lind,[1] Reza M. Baram,[2] and Hans J. Herrmann[2,3]
[1]*Institute for Computational Physics, Universität Stuttgart, Pfaffenwaldring 27, D-70569 Stuttgart, Germany*
[2]*Computational Physics, IfB, HIF E12, ETH Hönggerberg, CH-8093 Zürich, Switzerland*
[3]*Departamento de Física, Universidade Federal do Ceará, 60451-970 Fortaleza, Brazil*
(Received 11 November 2007; published 26 February 2008)

We generalize a recent study of random space-filling bearings to a more realistic situation, where the spacing offset varies randomly during the space-filling procedure, and show that it reproduces well the size distributions observed in recent studies of real fault gouges. In particular, we show that the fractal dimensions of random polydisperse bearings sweep predominantly the low range of values in the spectrum of fractal dimensions observed along real faults, which strengthen the evidence that polydisperse bearings may explain the occurrence of seismic gaps in nature. In addition, the influence of different distributions on the offset is studied and we find that a uniform distribution is the best choice for reproducing the size distribution of fault gouges.

DOI: 10.1103/PhysRevE.77.021304 PACS number(s): 45.70.−n, 46.55.+d, 61.43.Bn

I. INTRODUCTION

In the early 1990s the question of the possibility to tile an arbitrarily large strip of space-filling roller bearings without friction or slipping was addressed [1], motivated by the study of real systems such as seismic gaps. Seismic gaps are regions along a fault zone where earthquakes do not take place and therefore they could be explained by sheared plates on a space-filling bearing [2]. Fault zones or fault gouges are the interface regions between two tectonic plates in relative motion to each other and are typically self-similar [3]. The mechanical origin of the power law in the particle size distribution was associated with the particle's fracture probability which has been proposed to be controlled by the relative size of its nearest neighbors [3,4]. More recently, a geophysical model [5] explained the different values of the fractal dimension, ranging from $d_f=2.6$ to $d_f \simeq 3$, by taking into account the fault gouge strain. While such a model explains the dynamical origin of different power laws, there is still the question if the space-filling bearing scenario is able to reproduce such empirical results in a simple and systematic way. Bearings of disks or spheres are particular packings that resemble jammed packings [6] for a sufficiently large density, in the sense that the relative position between particles is fixed. However, the contact points are such that by rotating one single particle all particles can rotate without rubbing on each other—i.e., with no dissipation of energy similar to what occurs in seismic gaps. To have this property a simple coloring condition suffices for both disks or spheres, as explained below. Further, fault gouges present a broad range of particle sizes and corresponding densities [3], which appeals for a procedure to pack polydisperse sets of particles up to an arbitrary large density. Therefore, by reproducing with space-filling bearings the same particle size distributions observed in fault zones, one can strengthen the hypothesis that the existence of seismic gaps in fault zones may be related to the emergence of particular geometrical arrangements of their composing rocks, after local fragmentation due to the tectonic motion. Figure 1 illustrates two random space-filling bearings in two and three dimensions.

Pioneering studies with space-filling bearings were done using deterministic procedures in two [1] and three [7] dimensions and also using random algorithms [8]. However, up to now only specific initial configurations and fixed parameter values were addressed. In this paper we explore a subset of the phase space of possible space-filling bearings—namely, the one that can be constructed in the procedure described in Ref. [8]. The procedure is further developed below to construct realistic space-filling bearings in order to

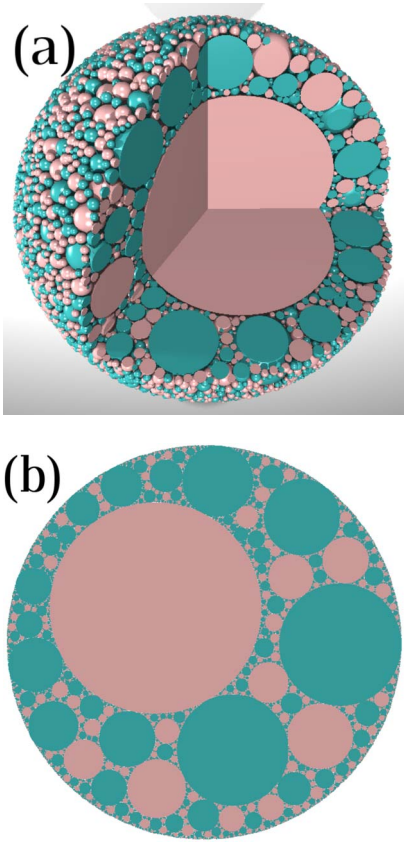

FIG. 1. (Color online) Illustration of a random space-filling bearing in (a) three and (b) two dimensions. Disks and spheres of the same color do not touch each other. The random space-filling bearing starts with a large disk or sphere, maximizing polydispersity (see text).

reproduce the range of fractal dimensions observed in fault gouges [3–5,9]. Our model is parametrized by a unique parameter that controls the strength of fragmentation and takes into account ensemble averages. Despite the wider freedom in the parameters and initial configurations, the system presents robust results in what concerns the fractal dimension. In particular, we will show that by varying the range of admissible values of the control parameter one finds fractal dimensions observed in fault gouges.

We start in Sec. II by describing in some detail the procedure to generate random space-filling bearings, introducing a parameter that accounts for fragmentation at the local scale. In Secs. III and IV we describe the results for two and three dimensions, respectively, with special emphasis on the size distribution and the fractal dimension. Discussions and conclusions are given in Sec. V.

II. RANDOM SPACE FILLING OF PARTICLES

In this section we will start by reexamining previous procedures [8] for constructing random space-filling packings and bearings and then introduce the necessary ingredients to obtain a fully random space-filling bearing.

Random bearings in two and three dimensions are constructed in the following way. First, one starts by randomly distributing a small number N_0 of disks or spheres within a given range of sizes, without touching each other. Second, one fills the empty spaces in the system by introducing iteratively the largest possible disk or sphere in the neighborhood of some empty region. Third, one resizes some disk or sphere in order for the packing to be bichromatic (bearing condition), i.e., only two colors are needed to color all disks in such a way that no disks of the same color touch each other. This guarantees the bearing condition: particles are able to roll on each other without friction or slipping. Figures 2(a) and 2(b) give illustrative examples of such random bearings in two dimensions.

The filling procedure is done by choosing randomly a void within the interdisk free space and then fitting the largest disk in it—i.e., fit the disk that touches the three nearest disks in the neighborhood, as illustrated in Fig. 2(a). For the three-dimensional case one considers spheres touching the four nearest neighbors.

The coloring procedure is done by attributing a proper color to the introduced disk. In the case that the three neighboring disks have the same color, one attributes the other color to the new disk. Otherwise, one chooses only one of the neighbors to be in contact with the new disk and the new disk shrinks to a size with radius $r=\alpha r_0$ $(0\leq\alpha\leq 1)$, where r_0 is the radius before shrinking, and gets a different color as the disk it touches. Figure 2(b) illustrates this coloring procedure.

Parameter α is our control parameter. For constant $\alpha=1$ one obtains the particular case where bearing cannot be guaranteed. In this case, frustrated contacts emerge when particles are forced to rotate [8], which would eventually lead to the fragmentation of the disks into smaller ones. Recently a method to implement realistic grain fracture in three-dimensional simulations of granular shear was proposed [10] based on breakable bonds between particles within a medium. We keep the model simple by using instead the reduction factor α, which mimics the effect of fragmentation: by shrinking a particle originally with frustrated contacts, we mimic its fragmentation into smaller particles that will fill the empty space left after the fragmentation.

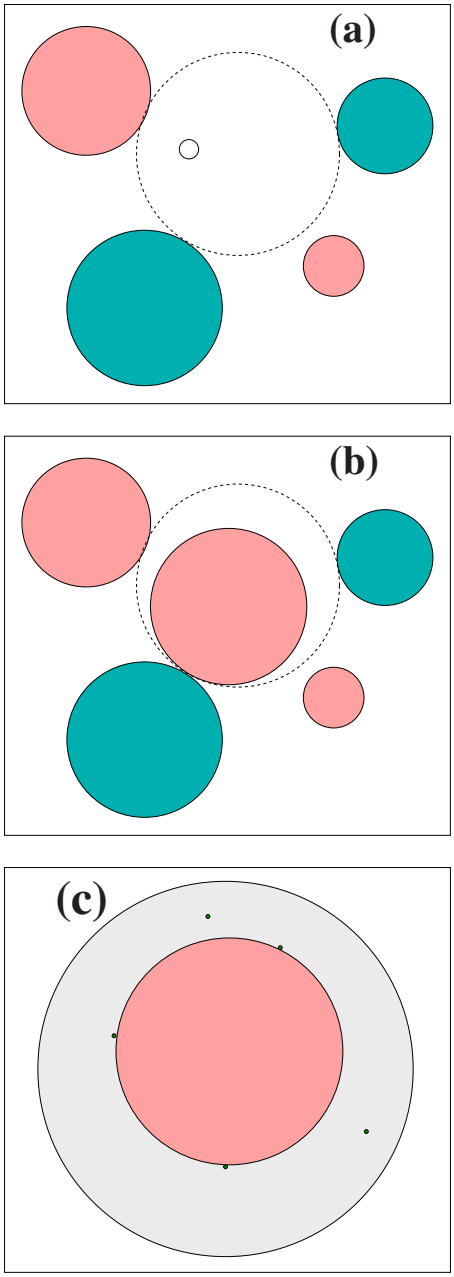

FIG. 2. (Color online) Sketch of the construction of a random space-filling bearing. (a) A new disk (solid circle) is randomly inserted in the system and is shifted and enlarged to the maximal accessible size (dashed circle) without overlapping neighboring disks. Then, (b) it is reduced by a factor $0<\alpha\leq 1$, keeping a single contact point with one of the neighbors and assuming the opposite color. (c) To start the space filling with a large disk one needs to place previously a few small "seeds" in the system and then proceed as in (a) and (b) (see text).

The algorithm described above was previously [8,11] used in two and three dimensions by fixing a given initial configuration with N_0 disks having sizes within a given fixed range and also by using a fixed reduction factor α during the filling and coloring stages. The density of the packing was studied as a function of the number N of existing spheres as well as the cumulative particle size distribution. It was found that the cumulative distribution obeys a power law—namely, $N(r) \equiv \int_r^\infty n(q)dq \sim r^{-d_f}$, where d_f is the fractal dimension of the bearing [12].

Next, we introduce the additional points to strengthen previous findings and improve the algorithm described above.

First, there is the statistical significance of the results and their sensitiveness to initial configurations—i.e., to the initial range $[r^* - \delta/2, r^* + \delta/2]$ of sizes. This initial configuration may influence the polydispersity of the system and consequently the attained distribution after filling the entire system. As we will see, a large number N_0 of initial disks typically influence how the density increases during the space-filling procedure.

To take this point into account we enable the construction procedure to start with an initial configuration having a single arbitrarily large disk (or sphere) and perform ensemble averages on a significant number of initial configurations. Concerning the single initial large disk, one should notice that it does not suffice for one single disk to introduce a second one, because in two dimensions each inserted disk needs to have at least three neighbors (four neighbors for three dimensions). However, as illustrated in Fig. 2(c), such a starting disk can be introduced into the system by previously distributing a few very small "seed disks" in the system and then following the algorithm described above. The number of such seeds is small, and therefore they do not affect significantly the cumulative size distribution. Their role is that the average distance between them is eventually of the order of the system size, enabling the introduction of a first disk with the size of the order of the system size. Of course, depending on the number and distribution of the seeds, the first initial disks may have also a size within the initial range of sizes. In this way, one generalizes the previous procedure [8] and maximizes the admissible polydispersity.

Second, we also introduced a criterion to increase computational efficiency of our algorithm. The neighborhood where the neighboring disks (or spheres) are searched for must be chosen conveniently. We propose to choose a size that decreases with the increase of the density ρ, since the denser the packing, the smaller the empty spaces into which to put new disks. Therefore, the radius r_n of the neighborhood of a given random point introduced in the system at iteration n is updated as $r_n = \frac{1-\rho_n}{\rho_n}(r_{sys} - r_{\max})$, where r_{sys} and $r_{\max}$ are the radii of the system and of the largest disk or sphere in it, respectively.

Third, we also consider the control parameter α to vary randomly within a tunable range of values. In particular, we argue that although a tentative value of the constant α could be obtained by analyzing samples of gouges in real situations, one expects that a certain range of admissible values for α is the most realistic assumption. Indeed, we show that the typical range of fractal dimensions observed in real fault gouges is in this way reproduced.

III. TWO-DIMENSIONAL CASE

We start this section by addressing the two-dimensional random space-filling bearing and systematically reviewing the behavior of the packing for different, but fixed, values of α and study the effect of fixed initial size ranges (no maximal admissible polydispersity). Figure 3 shows for this case the density $\rho(N)$ and cumulative size distribution $N(r)$ of two-dimensional random space-filling packings.

Figure 3(a) shows the density ρ as a function of the number N of disks for $\alpha = 1.0$ (packing) and also for $\alpha = 0.2$ and 0.6 (bearings) separately, starting from $N_0 = 40$ disks with radius in the range $\left[r^* - \frac{\delta}{2}, r^* + \frac{\delta}{2}\right]$ having $r^* = 0.11$ and $\delta = 0.06$. As expected, the convergence $\rho \to 1$ as N increases is faster for larger values of α. We consider one fixed initial configuration with N_0 initial disks, and therefore the different curves coincide for $N < N_0$.

In Fig. 3(b) we plot the distribution of the radius r of the disks, where $r_m = r^* - \frac{\delta}{2}$ is the minimal radius of the initial set of disks and the deviation from the power law for $r > r_m$ is due to the initial configuration. Below this value r_m, the size distribution obeys a power law $N = br^{-d_f}$, where d_f is the fractal dimension of the packing, plotted in the inset as a function of α (symbols). As one sees from the inset, the fractal dimension typically takes values in the range $1.2 < d_f < 1.4$, differently from the values found in two-dimensional cuts of fault gouges ($\sim 1.6 \pm 0.1$). There is a maximum of d_f for $\alpha = 0.5$ that can be explained from the definition of α in the algorithm described above. For a $\alpha < 0.5$, to each new disk introduced there is a remaining free space characterized by $\alpha' > 0.5$ such that $\alpha + \alpha' = 1$ and similarly for $\alpha > 0.5$.

Both Figs. 3(a) and 3(b) consider the same initial configuration. To study the influence of the initial configurations, we plot in Fig. 3(c) the density $\rho(N)$, fixing $\alpha = 0.6$, similar to previous works [11], and using different size ranges for the initial sets of $N_0 = 40$ disks—namely, in $[0.05R, 0.10R]$, $[0.15R, 0.20R]$, and $[0.20R, 0.25R]$—i.e., ranges with the same width $\delta = 0.06$, but centered around different values—namely, around $r^* = 0.075$, 0.175, and 0.225, respectively.

Since different initial configurations are now used, the density is no longer the same below N_0 as in Fig. 3(a). Further, one observes that the density converges to 1 for an increase of the value of r^*. In the inset the density $\rho(N)$ is plotted by fixing $r^* = 0.075$ and starting with an initial configuration having different widths—namely, $\delta = 0.2$, 0.4, 0.6, and 0.8. In these cases the density gives always similar dependences on N. Therefore, the average size r^* of the initial configuration is the important parameter to tune the density of the packing. Its width can be varied without changing significantly the results.

In Fig. 3(d) we plot the accumulative size distribution $N(r)$ of the disks for the same conditions as in Fig. 3(c). The value of the exponent remains almost constant, $d_f \sim 1.35$. In other words, the fractal dimension is not very sensitive to the initial configuration and the parameter on which the fractal dimension depends more strongly must be indeed α.

Since α is also the parameter controlling the fragmentation of disks with frustrated contacts (see above), we will

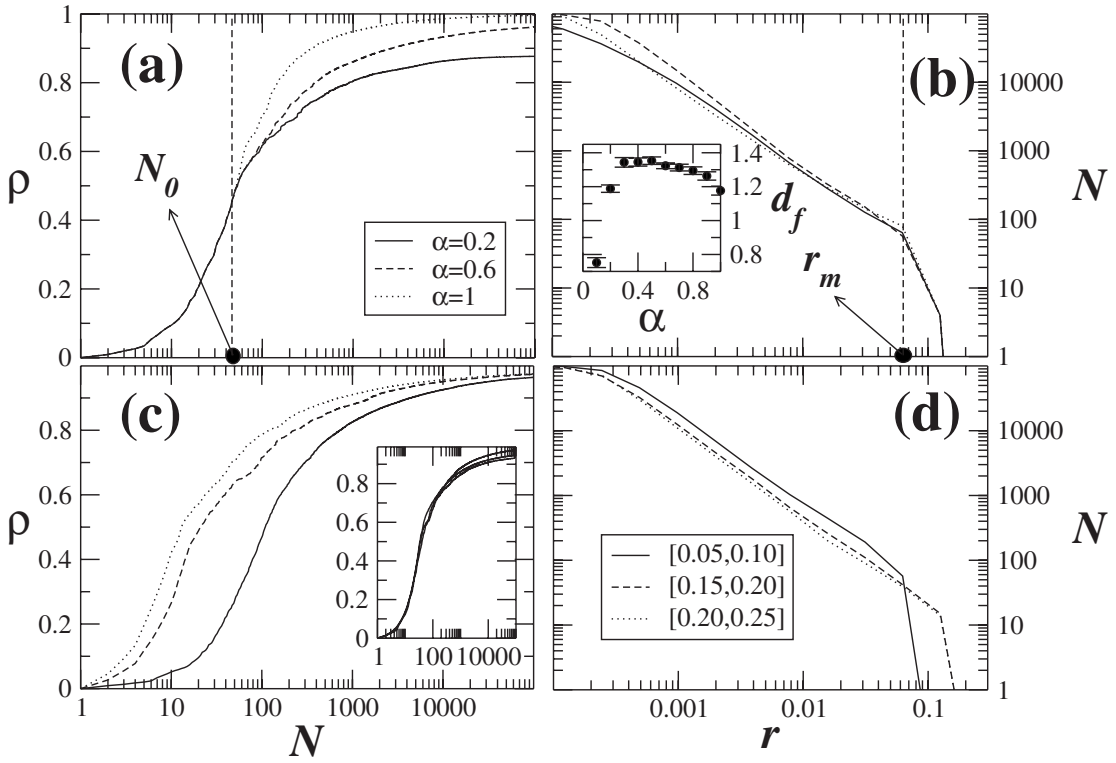

FIG. 3. Density and size distribution in two-dimensional random space-filling packings. (a) Density ρ of the packing as a function of the total number of disks N for different values of $\alpha=0.2$, 0.6, and 1.0, together with (b) the distribution of the radius r of the disks. In both cases, one starts from a fixed initial configuration of $N_0=40$ disks with radius in the range $[0.08R,0.14R]$ with $R=1$ being the radius of the system [see Fig. 1(b)]. The minimal radius of the initial set of disks is indicated as $r_m \sim 0.08$ (see text). Fitting of the power-law range in (b), the distribution $N(r)=br^{-d_f}$ yields the fractal dimension d_f as a function of α plotted in the inset. In (c) one plots the density as a function of N for the initial sets of $N_0=40$ disks in $[0.05R,0.10R]$, $[0.15R,0.20R]$, and $[0.20R,0.25R]$—i.e., ranges with the same interval width, but centered around different values—namely, around $r^*=0.075$, 0.175, and 0.225, respectively, and fixing $\alpha=0.6$. In the inset of (c) the density $\rho(N)$ is plotted for initial ranges $\left[r^*-\frac{\delta}{2},r^*+\frac{\delta}{2}\right]$ having the same center $r^*=0.075$, but different widths $\delta=0.2$, 0.4, 0.6, and 0.8. In (d) we plot distribution $N(r)$ of the spheres as a function of r for the same conditions as in (c). In all cases $N=10^5$ disks.

now study it more deeply. When α is able to vary randomly, the fragmentation of the largest disk in the free holes can be regarded as a random process by its own. We next consider α to be each time randomly selected from a fixed interval $[\alpha^*-\Delta\alpha/2,\alpha^*+\Delta\alpha/2]$. We will show that when enabling α to take different values for each particle shrinking, one obtains fractal dimensions similar to the ones observed in fault gouges [3–5].

To this end, we put everything together—namely, α varying in the middle range of admissible values, a large initial disk, and an ensemble average over a significant number of initial configurations. The results for the density and size distributions are shown in Fig. 4, where one considers three initial seeds in the range $r_M=2r_m\sim R/1000$, with R the size of the system and α varies randomly in the range $[0.5-\Delta\alpha/2,0.5+\Delta\alpha/2]$. Averages are over a sample of 100 initial configurations. Since the initialization, filling, and coloring procedures are now all random, we call these systems fully random space-filling bearings.

Figure 4(a) shows the density as a function of the number N of disks for $\Delta\alpha=0.2$, 0.4, 0.6, and 0.8. One sees an abrupt transition above $N=3$ (initial seeds), due to the introduction of the first large disk. For all four cases the dependence of ρ on the range of α values is similar, with the convergence toward $\rho=1$ being slightly slower for narrower ranges, because they hinder the occurrence of large disks.

Figure 4(b) shows the size distribution $N(r)$ for each of the four ranges. All the distributions almost coincide, as shown in the inset where the fractal dimension d_f taken from $N(r)\sim r^{-d_f}$ is almost constant ($d_f\sim 1.54$). This value is larger than the one obtained when α is kept constant (see Fig. 3). Notice that the value of the fractal dimension for $\Delta\alpha=0$, though corresponding to the case of constant $\alpha=0.5$, is different from the one plotted in the inset of Fig. 3(b), since the constructing procedure of the bearing is slightly different (see Sec. II).

Since the above value is obtained from a significantly larger sample of initial configurations and all the parameters α and position of the disks are randomly selected, we will consider this value $\bar{d}_f=1.54$ as the characteristic exponent of the size distribution for fully random two-dimensional space-filling bearings. The average characteristic value $\bar{d}_f=1.54$ obtained lies in the range of values measured of the fractal dimension measured in real fault gouges ($D=1.6\pm0.1$) [3,4], as indicated with a dashed line and shadow region in the inset of Fig. 4(b).

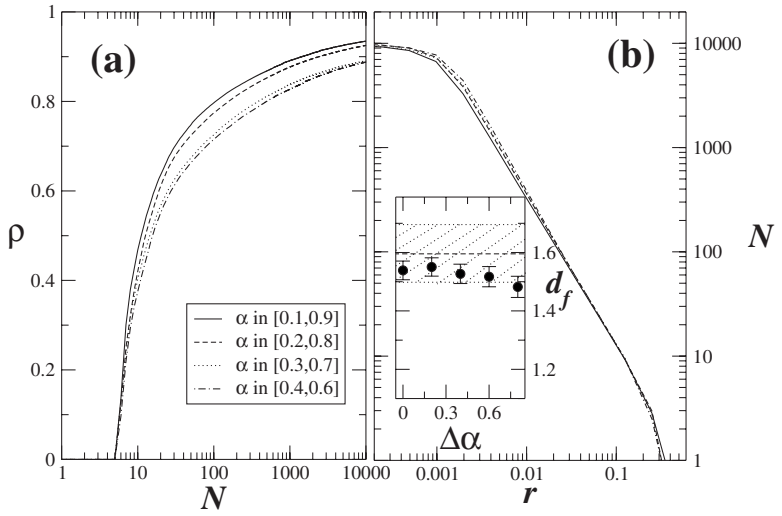

FIG. 4. Averaging (a) the density ρ and (b) the distribution size $N(r)$ over 100 initial configurations starting from large disks ($r \sim R/2$) and with α varying in a range $[0.5-\Delta\alpha/2, 0.5+\Delta\alpha/2]$ with $\Delta\alpha=0.2$, 0.4, 0.6, and 0.8. The inset of (b) shows that the fractal dimension in $N(r) \sim r^{-d_f}$ is almost independent of $\Delta\alpha$, yielding $d_f \simeq 1.54$, which is within the numerical errors of real fault gouges (see text).

Until now, the value of α was considered to vary *uniformly* within a certain range of values. If the probability distribution for choosing α values is Gaussian, similar results are obtained, where the standard deviation σ of the distribution plays a similar role as the width $\Delta\alpha$ used in Fig. 4.

However, if we take values within a range, say, $\alpha \in [0.1, 0.9]$, and chose them according to a power-law distribution $P(\alpha) \sim \alpha^{-\beta}$, the fractal dimension changes significantly, as shown in Fig. 5. Even for small values of the exponent β—e.g., $\beta=0.5$—the fractal dimension decreases when compared to the value obtained for the uniform distribution ($\beta=0$) and remains approximately constant at $d_f \sim 1.43$.

Notice that $\beta=0$ in Fig. 5 corresponds to $\Delta\alpha=0.8$ in Fig. 4(b). If the power-law distribution selects values in a range with a different width, a similar decrease of the fractal dimension is observed when comparing with the uniform distribution case. Therefore, one can conclude that a reasonable choice for constructing space-filling bearings with fractal dimension similar to the one observed in fault gouges is by taking a random value of α uniformly distributed in a certain range around 0.5.

IV. THREE-DIMENSIONAL CASE

As described above in Sec. II, a three-dimensional version of fully random space-filling bearings is obtained in a similar way as for disks with the single difference that the introduction of new spheres takes into account four nearest neighbors. In this section we address the case of three-dimensional space-filling bearings as a more realistic approach to fault gouges and study how well the two-dimensional model approximates three-dimensional systems of spheres.

Recently [10], it was found that grain fracture simulations produce a comminuted granular material similar to the one observed in real fault gouges. From those simulations, it followed that the comminution rate and survival of large grains is sensitive to applied normal stress, with a fractal dimension of the resultant grain size distributions in the range $d_f \in [2.3 \pm 0.3, 2.9 \pm 0.5]$, which agrees with the observations of three-dimensional samples of real gouges where typically $d_f \sim 2.58$.

In three-dimensional space-filling bearings with a constant value of α the fractal dimension lies above the observed values in fault gouges. In Fig. 6 we plot typical values of d_f as a function of α. The fractal dimension of such bearings is typically larger than $d_f \gtrsim 2.58$ (dashed line) with values within the range $d_f \in [2.60 \pm 0.10, 2.74 \pm 0.15]$ and, similarly to the two-dimensional case, the maximum of d_f is reached for $\alpha \sim 0.5$.

As summarized above in the Introduction, it was recently found [5] that fractal dimensions ~ 2.6 are observed for low-strain gouges. In regions subject to larger shear strain the fractal dimension is significantly larger, $\lesssim 3$. Therefore, the particle size or mass dimensions were proposed as a way to distinguish between regions with different strain strengths [5]. From Fig. 6, one sees that a similar range of values for the fractal dimension is also found for space-filling bearings.

Furthermore, the explanation relating the fractal dimension of fault zones and their strain strength assumes that

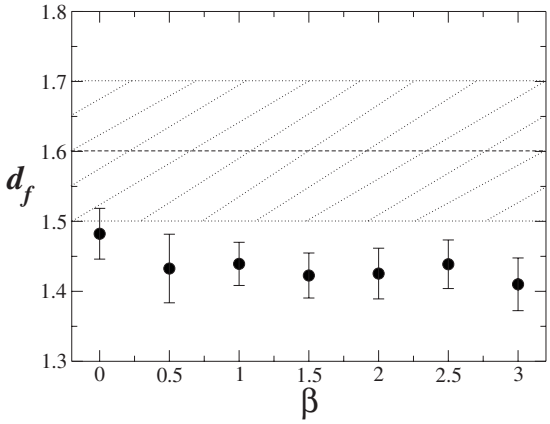

FIG. 5. The fractal dimension as a function of the exponent β when the value of α is chosen according to a power law $P(\alpha) \sim \alpha^{-\beta}$ in a range $\alpha \in [0.1, 0.9]$. Although within the error bars, the fractal dimension is somewhat lower compared to Fig. 4(b) where the distribution of chosen α values is uniform (see text).

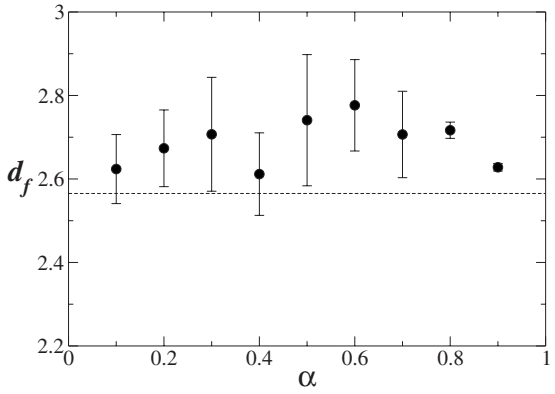

FIG. 6. The fractal dimension as a function of α for three-dimensional random space-filling bearings when α is kept constant. A similar procedure as the one illustrated in Fig. 2 is used, with new spheres being introduced touching the *four* nearest neighbors (see text). The dashed line indicates one typical value $d_f \sim 2.58$ found in some real fault gouges [10].

fragmentation is controlled by nearest-neighboring particle contact and that a particle is most likely to split into smaller particles with a particle of similar size, yielding a larger fractal dimension ~3. In the case of our construction procedure for space-filling bearings, this would correspond to the case of $\alpha \sim 0.5$. Indeed, from Fig. 6 one observes that the maximum of the fractal dimension is reached for such α values yielding $d_f = 2.74 \pm 0.15$.

We vary α randomly in a range around 0.5 and study the dependence of the space-filling bearing on the width $\Delta\alpha$ of the range $[0.5-\Delta\alpha/2, 0.5+\Delta\alpha/2]$. In Fig. 7(a) one sees that the density increases faster for larger $\Delta\alpha$, similarly to what was shown in Fig. 4(a). As for the fractal dimension, Fig. 7(b) shows that it decreases slightly when compared with the case of constant α ($\Delta\alpha=0$). Therefore, increasing the width $\Delta\alpha$ of the range of admissible values for α one is able to reduce the fractal dimension of the bearing.

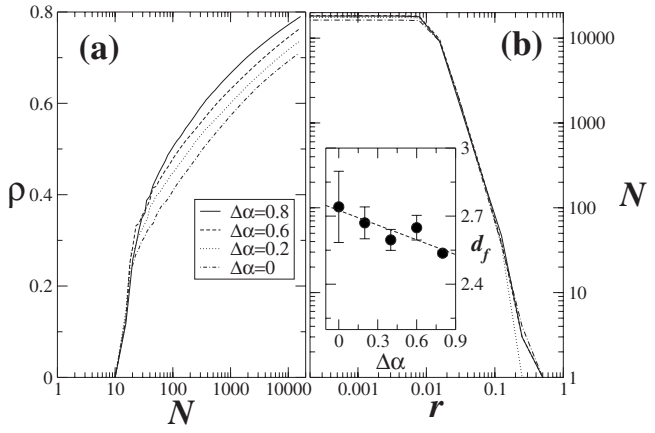

FIG. 7. Three-dimensional space-filling bearings for varying $\alpha \in [0.5-\Delta\alpha/2, 0.5+\Delta\alpha/2]$. (a) The density ρ as a function of the number N of spheres for $\Delta\alpha=0$, 0.2, 0.6, and 0.8 and (b) the corresponding size distribution $N(r)$ with the fractal dimension d_f in the inset. In all cases $N=10^4$.

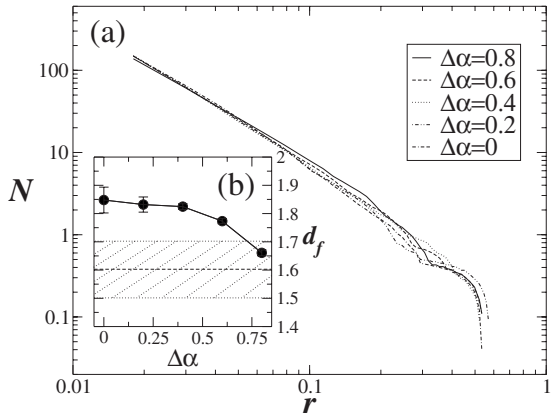

FIG. 8. (a) The size distribution of two-dimensional cuts of the three-dimensional space-filling bearings addressed in Fig. 7 and (b) the corresponding fractal dimension.

Similarly to the situation of measures taken in fault gouges, the two-dimensional cross section of such three-dimensional space-filling bearings should have a fractal dimension within the range of the observed empirical values in real fault gouges ($d_f = 1.6 \pm 0.1$ [3,4]). By averaging several different two-dimensional cross sections of the three-dimensional bearings, we plot in Fig. 8(a) the size distribution of a typical two-dimensional cross section for different values of $\Delta\alpha$. In Fig. 8(b) we observe that only for very wide ranges of α values is it possible to obtain a fractal dimension similar to the one observed on fault zones.

V. DISCUSSION AND CONCLUSIONS

In this work we studied the size-distribution of random space-filling bearings with large polydispersity, showing that it reproduces well the size distribution found in fault gouges. Focusing on the dependence of the bearings' fractal dimension on the spacing offset, we have shown that the fractal dimensions of such bearings sweep the low range of values observed in real faults. Since recently it has been reported that the fractal dimension varies in space along fault gouges [5], our findings enable us to conjecture that the occurrence of seismic gaps, where earthquakes are absent and therefore behave similarly to roller bearings, may occur in regions where the fractal dimension lies in the low range of admissible values—namely, $d_f \in [2.5, 2.75]$.

To compute an accurate value for the exponent characterizing random bearings, we introduced a general algorithm that allows α to vary randomly in a wide range of admissible values, typically $0 < \alpha < 1$, and start the space-filling procedure from one unique large disk (or sphere), maximizing the range of admissible sizes in the bearing.

With such a model we were able to show that bearings have a fractal dimension with values within the range of values in a real fault. Since it is known [5] that along a specific fault gouge the fractal dimension varies typically between ~2 and ~3, our results support the hypothesis that seismic gaps, occurring only in certain particular locations of the fault, could be explained by this simple geometrical model.

Further, we also interpret the control parameter α for the bearing property as a measure of the fragmentation strength and introduce simple criteria to improve the computational efficiency of previous space-filling packing algorithms.

To improve further our findings we should also take the effect of gravity into account. Moreover, concerning the algorithm by itself, some further properties due to the *ad hoc* procedures could be analyzed. Namely, the study of the influence of correlations and constraints that emerge due to the sequential character of the algorithm should help one to understand the range of observed fractal dimensions. These and other points will be addressed elsewhere.

ACKNOWLEDGMENTS

The authors thank Bibhu Biswal for useful discussions. This work was supported by the Deutsche Forschungsgemeinschaft, under Project No. LI 1599/1-1.

[1] H. J. Herrmann, G. Mantica, and D. Bessis, Phys. Rev. Lett. **65**, 3223 (1990).
[2] J. A. Astrøm, H. J. Herrmann, and J. Timonen, Phys. Rev. Lett. **84**, 638 (2000).
[3] C. Sammis, G. King, and R. Biegel, PAGEOPH **125**, 777 (1987).
[4] C. Sammis and R. Biegel, PAGEOPH **131**, 255 (1989).
[5] C. G. Sammis and G. C. P. King, Geophys. Res. Lett. **34**, L04312 (2007).
[6] A. Donev, R. Connelly, F. H. Stillinger, and S. Torquato, Phys. Rev. E **75**, 051304 (2007).
[7] R. Mahmoodi Baram, H. J. Herrmann, and N. Rivier, Phys. Rev. Lett. **92**, 044301 (2004).
[8] R. Mahmoodi Baram and H. J. Herrmann, Phys. Rev. Lett. **95**, 224303 (2005).
[9] S. Roux, A. Hansen, H. J. Herrmann, and J.-P. Vilotte, Geophys. Res. Lett. **20**, 1499 (1993).
[10] S. Abe and K. Mair, Geophys. Res. Lett. **32**, L05305 (2005).
[11] R. Mahmoodi Baram and H. J. Herrmann (unpublished).
[12] S. S. Manna and H. J. Herrmann, J. Phys. A **24**, L481 (1991).